

N + N → N₂ Reaction Rates on Rh(111)

DAVID N. BELTON,* CRAIG L. DIMAGGIO,* AND K. Y. SIMON NG†

**Physical Chemistry Department, General Motors Research, Warren, Michigan 48090,
and †Department of Chemical Engineering, Wayne State University, Detroit, Michigan 48202*

Received April 21, 1993; revised June 25, 1993

We have studied the reaction of N atoms adsorbed on Rh(111) to make gas phase N₂, using a combination of temperature programmed desorption and kinetic modeling. Electron beam dissociation of adsorbed NO was used to prepare surfaces with the highest N atom coverages (≈0.5 monolayer) yet reported. Surfaces with coadsorbed N and O were also studied. Our experiments and modeling show that N atoms desorb as N₂ from Rh(111) in at least three distinct desorption states with reaction rates that vary by about four orders of magnitude. Comparison of the N₂ formation rates reported here with those measured during reaction of CO and NO at 16 Torr shows that under reaction conditions the surface most likely has an intermediate coverage of nitrogen atoms. In addition, our results show that at high N atom coverages N₂ is formed at least 50× faster than under reaction conditions, indicating that N atom recombination is not the rate limiting step in the reduction of NO by CO over Rh(111). © 1993 Academic Press, Inc.

1. INTRODUCTION

Rh is virtually irreplaceable in the current generation of automotive catalytic converters, primarily because of its superior activity in the reduction of nitrogen oxides (NO_x) to nitrogen (1–3). However, because of the cost of Rh and availability considerations, it is unlikely that the amount of Rh in current catalysts can be increased to meet future standards which will require both lower NO_x emissions and greater catalyst durability. One part of our effort to utilize Rh more effectively focuses on the kinetics of NO_x reactions over Rh single crystals. By studying such a well-defined model catalyst we are able to specify with a high degree of certainty the rates and product distributions for important probe reactions. In a previous paper we reported the reaction rates and product distributions for the CO + NO reaction over Rh(111) at moderate pressures (1–100 Torr) (4). In that paper we concluded that the mechanistic details for the reaction could not be specified with a high degree of certainty due to the lack of good rate constants for N atom reactions on Rh(111).

In this paper we focus on the N_a + N_a → N₂^{gas} reaction on Rh(111). Our goal is to generate a rate expression which describes the N₂ formation rate over a wide range of N atom coverages. We emphasize reaction in the high coverage regime because previous papers suggest that relatively high N coverages are present during reaction at moderate pressures (20 Torr) (5, 6).

The experiments we report here fill an important gap in the understanding of N atom reactions on Rh(111). Much has been written on the interactions of NO with Rh single crystals (7–10) and with planar Rh model catalysts (11, 12); however, to our knowledge no one has reported a rate constant for the N + N reaction (k_{N+N}) at N coverages (θ_N) above 0.25 monolayer (ML), without complications due to other surface reactions (e.g., NO dissociation), and in the absence of other surface species (e.g., oxygen). The latter condition is appropriate since CO oxidation proceeds at a rate that is at least as fast as N₂ formation on these surfaces (5, 6), which leads to low oxygen coverages. These three qualifying conditions are important because they are the pre-

ferred conditions for the determination of rate constants that can be applied to reactions at higher pressures. Currently, the best estimation of k_{N+N} is for low coverages of N atoms generated by thermal dissociation of NO during an NO TPD (9). Relatively low coverages of N atoms are obtained in this NO TPD experiment because up to half of the nitrogen desorbs from the surface as NO instead of dissociating to give N atoms. These results are a helpful starting point to our understanding of the reactions of NO over Rh surfaces; however, it is very difficult to extract a rate constant for high N coverage from NO TPD data for several reasons. First, during an NO TPD experiment at least three processes can take place at temperatures where high N coverages desorb: NO desorption, NO dissociation, and N₂ desorption. When three reactions occur in the same temperature range, independent determination of the rate constant for a single reaction is difficult (this is not a problem at low NO coverage where N recombinatively desorbs at a temperature where no other reactions occur). Second, it is known that adsorbed oxygen (from NO dissociation) alters N + N recombination rates on Rh(111) (9). Finally, N coverages obtained during NO TPD are about half of those predicted in previous papers which modeled the CO + NO reaction rates at moderate pressures (10–100 Torr) (5).

In order to improve upon previous estimates of k_{N+N} , we have prepared N atoms on Rh(111) via electron beam dissociation of NO. In this way we have been able to make clean N atom coverages of up to 0.5 ML (N atoms/surface Rh). Using a combination of TPD and simple kinetic modeling we show that N atoms recombine and desorb from Rh(111) in three different states. We also calculate desorption rate constants for each state. In addition, we compare our data to previous results for the CO/NO reaction (4), giving some insight as to what the surface N is like under moderate pressure reaction conditions.

2. EXPERIMENTAL ASPECTS

2.1. Apparatus

The experiments were performed in a standard ion-pumped vacuum system similar to that described elsewhere (13). The system is equipped with a double pass cylindrical mirror analyzer for Auger electron spectroscopy (AES), a four grid LEED system, a high resolution electron energy loss (HREELS) spectrometer, and an apertured quadrupole mass spectrometer (QMS) for temperature programmed desorption (TPD). The Rh(111) surface was oriented to within 1° of the desired crystallographic direction and polished with $\frac{1}{4}$ μm diamond polish prior to mounting. The sample was mounted with Ta wires spot-welded on the back of the crystal to allow for resistive heating and LN₂ cooling. The crystal was cleaned with cycles of sputtering at 875 K using 2 KeV Ar ions followed by annealing to 1350 K until all AES detectable contaminants (except carbon) were removed and sharp LEED patterns were obtained. At that point the C was removed by slow cycling under a flux of O₂ between 800 K and 1250 K. This procedure removed C from both the surface and the near surface regions of the crystal. Subsurface C migrates to the surface at high temperatures, reacting with surface O atoms to make CO (14). All TPD spectra were taken with the crystal placed about 2 mm from the aperture of the QMS. The sample was heated at 10 K/s and nine masses were obtained simultaneously during the experiment.

2.2. N Atom Preparation

In order to obtain high N atom coverages, four thoriated iridium filaments were mounted in parallel on Ta posts to provide electrons to bombard preadsorbed NO on Rh(111). Typically, NO was admitted through a doser, raising the background pressure by 5×10^{-11} Torr. The Rh(111) crystal was held at 120 K and, when it was in front of the doser, a saturation NO coverage was achieved within 30 sec. Next the sample

was placed about 5 mm from the electron source with a +100 V bias applied to the sample and the filament current adjusted so that 1.2 mA of current was passed to the Rh(111) crystal for 5 min. During bombardment the sample temperature increased from 120 to 150 K. When the sample was examined with AES after e^- beam bombardment, we found that most of the oxygen had been removed from the surface. The high N/O ratio (≈ 8 N per O) indicates significant NO dissociation occurs during bombardment and that the dissociation occurs via electron stimulated desorption of oxygen. Next, the sample was heated to at least 415 K (higher temperatures if lower N coverages were desired) to remove any residual NO that might remain on the surface. TPD experiments confirm that no NO desorbs from the e^- beam bombarded surfaces; however, we suspect that if a small amount of NO remained after e^- beam bombardment it would dissociate during the TPD experiment. Finally, we used adsorbed CO to clean off (via CO₂ formation) the oxygen contamination that might still be present. The oxygen cleaning procedure was as follows: (1) about 3 Langmuirs of CO was dosed at 120 K, (2) the surface was heated to at least 415 K (higher if lower N coverages were desired), (3) the surface was cooled to 120 K, and the process repeated. We estimate that under the worst conditions residual oxygen coverages were approximately 0.05 ML (from AES and TPD) and residual CO coverages (which desorbs at lower temperatures than does N) were about 0.1 ML. To avoid conflicts of CO and N₂ signals in the QMS we monitored mass 14 as a measure of N₂ desorption.

3. RESULTS

3.1. N₂ Desorption from N Adsorption

Figure 1 shows the TPD data for a series of different N coverages on Rh(111). Using our N atom preparation method, the maximum amount of adsorbed N obtainable is 0.49 ML (+0.18/−0.15 ML). This maximum coverage was limited because we had

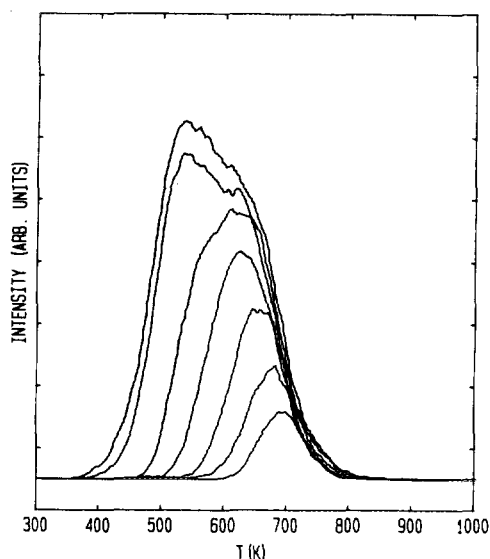


FIG. 1. N₂ desorption from N adsorbed on Rh(111) by electron beam dissociation of adsorbed NO. The N coverages in ML are 0.04, 0.08, 0.13, 0.20, 0.31, 0.44, 0.49.

to heat to at least 415 K in order to remove residual NO and scrub off undesirable oxygen using CO (see Section 2.2). N atom coverages were estimated by comparison of the N₂ TPD area of Fig. 1 to N₂ desorption data from saturation NO TPD data taken under the same conditions as those in Fig. 1. We rely on a previous paper by Root *et al.* (9) which reported that 0.37 ML of N atoms desorb as N₂ after the heating of a saturation NO layer sufficient to remove molecular NO (495 K). We assign a relatively large error ($\pm 33\%$) to our method of coverage calibration (see Section 4.1.3).

In Fig. 1 at the lowest coverage (0.045 ML) we detect a single N₂ desorption peak (state I) which has a desorption maximum of 695 K. As the N coverage is increased the peak maximum for state I shifts to lower temperatures and broadens significantly. At $\Theta_N = 0.3$ ML a low temperature shoulder (565 K), indicative of a second desorption peak (state II), is detected. At still higher coverages state II increases in intensity shifts down to lower temperature (535 K) as a third unresolved state grows in.

3.2. Modeling of the $N + N \rightarrow N_2$

TPD Data

To obtain a reasonable rate expression and rate constants for the $N + N$ reaction, we have modeled the TPD data of Fig. 1. To model the TPD data we require (1) a rate equation which relates the desorption rate from a given state to the N coverage and the surface temperature, (2) estimates of the N atom coverage in each state, and (3) a simple computer program that calculates the desorption rate as a function of sample temperature, adjusts the surface N coverage according to the desorption rate, and then calculates the desorption rate at a slightly higher temperature.

3.2.1. Rate expression. We assume that the experimental data are composed of desorption rates from discrete desorption states. We approximate the desorption rate from each state as

$$-\frac{d\theta}{dt} = \frac{1}{\beta} \Theta_N^n \nu \exp[-(E_a - \alpha_N \Theta_N)/RT], \quad (1)$$

where $-d\theta/dt$ is the desorption rate, β is the heating rate, ν is the preexponential factor, Θ_N is the N coverage in that state, n is the reaction order, E_a is the activation energy, and α_N is the N coverage dependence of E_a . This formulation is a fairly standard variation of the commonly used Polanyi-Wigner model (15). One point to make is that we have chosen for the sake of simplicity, to express all of the coverage dependence of the rate constant in the activation energy. Our intention is not to suggest that this is necessarily the "correct" formulation of this rate equation; we merely put it forth as a reasonable expression through which to estimate the desorption rate.

3.2.2. Coverages. The N atom coverages are expressed in ML on a per Rh atom basis. We rely on the previously mentioned paper by Root *et al.* (9) in which they report that 0.37 ML of N (N atoms/surface Rh atom) desorb as N_2 during TPD of a saturation

layer of NO on Rh(111) heated to contain only atomic species. All of our N coverages were calibrated vs the amount of N_2 that desorbs after adsorption of a saturation layer of NO on Rh(111). We assign a relatively large amount of error to this method of coverage calibration (33%). Errors in the coverage calibration are the primary source for error in our calculation of the desorption rate constants.

3.2.3. Assumptions. Equation (1) has five adjustable parameters for each TPD peak. Our modeling shows that at least three peaks are present in Fig. 1; therefore, a complete model of the data has 14 adjustable parameters (the coverage in one of the three states is fixed by the coverage in the other two). Obviously, with 14 parameters good solutions abound and it is prudent to constrain the solution set in a reasonable manner. We do so by assuming (1) that all three states are second order with respect to N coverage ($n = 2$), (2) that higher temperature desorption states have higher activation energies than do lower temperature state (intuitively obvious, but not necessarily true if large differences in preexponentials are tolerated), (3) that α_N is greater for the low coverage states (this assumption is based on our observation that state I is the broadest of the three peaks and state III is the most narrow), and (4) that lower coverage states have lower preexponentials than do higher coverage states. This last assumption is based on transition state theory, which states that the preexponential factor is proportional to the exponential of ΔS between the free reactants and the reactants at the transition state (16). Our assumption is that ΔS is primarily due to loss of translational entropy, which is greatest for low N coverages. Under this assumption, it follows that ΔS is most negative at low N coverages, resulting in the lowest preexponentials. None of these constraints are required to fit the data, but they do serve to minimize the range of possible parameter values in the fit. Although a different set of assumptions leads to different rate parameters, this dif-

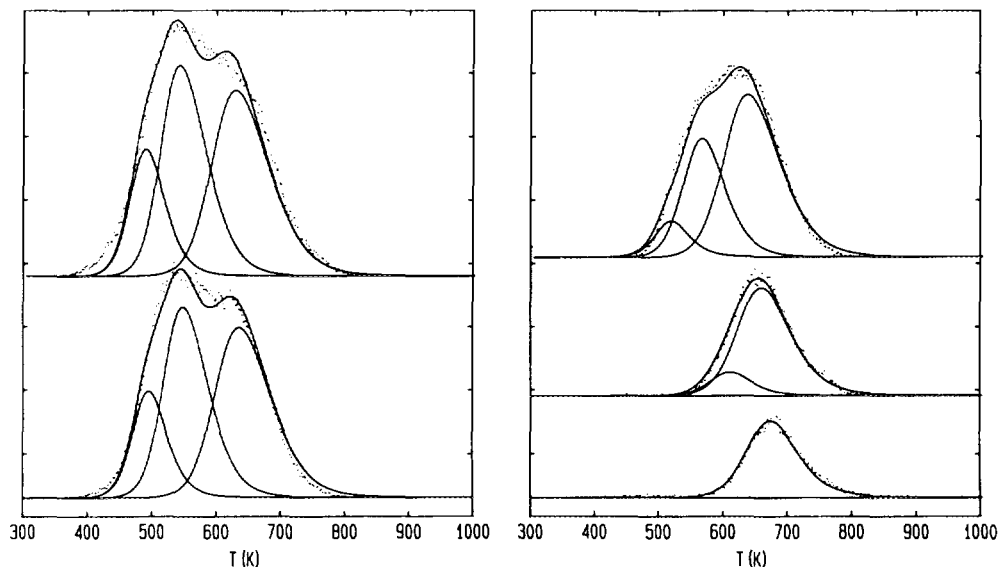


FIG. 2. Fits of the N TPD data of Fig. 1 using the model described in Section 3.2. The N coverages in ML are 0.08, 0.13, 0.31, 0.44, 0.49.

ferent set of parameters predicts the same reaction rate as do the ones we have generated.

We fit the TPD data as follows: First, we fit the data at very low coverage ($\Theta_N = 0.08$ and 0.045 ML) assuming a single desorption state (state I). These state I values were then applied to the data at higher coverage by adjusting only the state I coverage. Next we fit $\Theta_N = 0.135$ ML, assuming that both states I and II were present. This fit sets the rate constant for state II. Finally, we fit the remaining high coverage data to determine the state III parameters. Several iterations of fitting data at low and high coverage were used to converge on a single parameter set (three different states) that gave good fits for our entire data set. Spectra representative of the quality of fit obtained are shown in Fig. 2. The parameters used for the fits of the data are given in Table 1.

3.3. Filling of the TPD States

Figure 3 summarizes the amount of N that desorbs from each of the three states, θ_i , as a function of total N coverage on the sur-

face. The amount of desorption from each state is derived from the fits of the data shown in Fig. 2 and described in Section 3.2. In Fig. 3 the circles represent desorption from state I, the squares are for desorption from state II, and the triangles are from state III. The lines represent a smooth curve drawn through the data for each individual desorption state. The filled symbols are for N atom coverages prepared by electron beam dissociation of NO (Section 2.2) and the open symbols are the two surfaces prepared by thermal decomposition of NO (see Section 3.3.1). Comparison of the open and closed symbols shows that the filling of the three states is not strongly dependent on our method of N atom preparation.

Figure 3 shows that state I fills first and appears to saturate at a maximum of about 0.2 ML of N. State II begins to fill at a total N surface coverage of about 0.10 ML, with roughly 0.2 ML of N desorbing in this state when the initial N coverage is 0.5 ML. State III is the third state to fill, with about 0.075 ML of N desorbing in this state when the initial N coverage is 0.5 ML.

TABLE I
Rate Constants for N₂ Desorption from Rh(111)

State	E_a kcal/mol	ν N ₂ /Rh site-sec	α_N kcal/mol-ML N	β_O kcal/mol-ML O
I	35.7	5.0×10^{11}	10	17
II	32.6	4.0×10^{12}	9	≈ 0
III	29.0	1.2×10^{13}	7.5	≈ 0

3.4. Effects of Oxygen

3.4.1. Preparation of the N plus O surfaces. To sort out the effect of O on N₂ desorption rates, we performed three experiments which compared desorption of N as N₂ from surfaces with and without oxygen present. In Figs. 4a (0.11 ML) and 4c (0.22 ML) we show data for relatively low coverages of N atoms without surface oxygen present. Thermal decomposition of NO was used for these experiments because this method is convenient for preparing surfaces with one O atom per N atom. The oxygen-free surfaces were prepared as follows: (1) a low coverage of NO was adsorbed at 120 K, (2) the surface was heated to 425 K to dissociate the NO, (3) then CO was adsorbed at 120 K and the surface heated to

425 K (removing O as CO₂). This process was repeated three times. For surfaces with equal amounts of N and O (Figs. 4b and 4d), step (3) of the procedure was omitted. This thermal NO dissociation procedure (where the temperature is below the N₂ desorption threshold) gives surfaces with equivalent N and O coverages of 0.09 ML (Fig. 4b) and 0.20 ML (Fig. 4d).

The high N coverages shown in Figs. 4e and 4f could only be prepared by e^- beam dissociation of a saturation NO exposure. Preparation of the oxygen free surface is described in Section 2.2. For the case with oxygen, after electron beam dissociation of NO, the surface was heated to 440 K, then cooled to 120 K, and then approximately 50 liters of O₂ were dosed in an attempt to adsorb as many O atoms as possible. For the data shown in Fig. 3f we estimate an N coverage of 0.47 ML and an O coverage of 0.1 ML (estimated by the downshift of the high temperature desorption edge).

3.4.2. Oxygen induced changes in the N TPD data. Looking first at the lowest N coverages we studied, without oxygen present on the surface, 0.11 ML of N desorbs primarily out of state I with a small amount of desorption from state II. These two peaks overlap to give a desorption maximum at 670 K. When a surface is prepared with 0.09 ML of O and 0.09 ML of N we find that the N₂ desorption rate peaks 40 K lower at 630 K, which results in a pronounced shift of 30 K in the high temperature edge of the desorption peak. A secondary effect is seen as a subtle change in the peak shape which

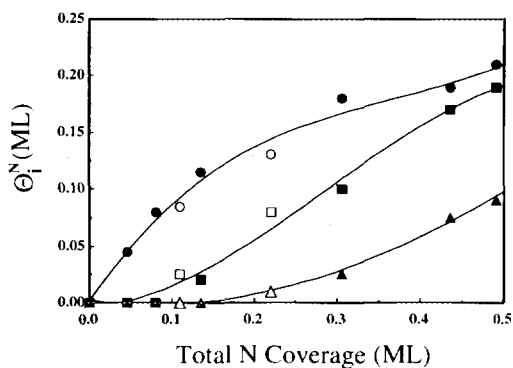


FIG. 3. Distribution of N atoms to individual desorption states as a function of the total surface N coverage. Circles are for state I desorption, squares are for state II, and triangles are for state III. Open symbols are for surfaces prepared by thermal dissociation of NO and filled symbols are for e^- beam dissociation.

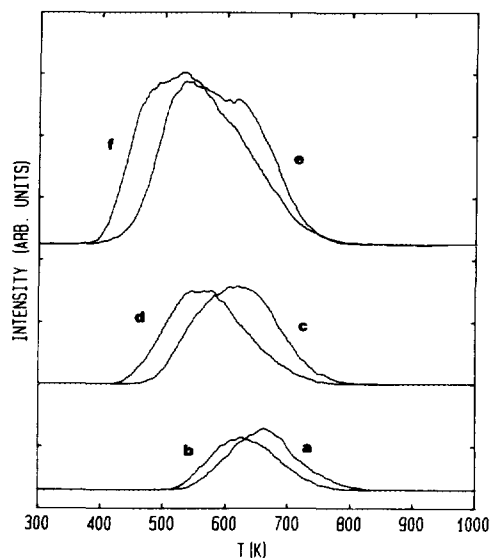


FIG. 4. Effect of oxygen on N₂ desorption from N adsorbed on Rh(111). Figures 4a, 4c, and 4e are data for surfaces without oxygen where the N coverages are (a) 0.11 ML, (c) 0.22 ML, and (e) 0.49 ML. Figures 4b, 4d, and 4f are data for surfaces with both N and O where coverages in ML are (b) 0.09 N: 0.09 O, (d) 0.20 N: 0.20 O, (f) 0.47 N: 0.10 O.

indicates a change in relative populations of the two states.

In Figs. 4c and 4d, we examine the effect of increased O and N coverage. Figure 4c shows the desorption data taken from 0.22 ML N without surface oxygen present. The peak maximum is at roughly 620 K. When desorption data were taken from a surface with 0.20 ML of N and 0.20 ML of O, the peak maximum and the high temperature edge shifted down by 55 K and the peak shape changed.

At the highest surface N atom coverages, we were unable to achieve comparable N and O atom coverages. Thus in Fig. 4f, $\Theta_N = 0.47$ ML but we estimate that $\Theta_O \approx 0.1$ ML. However, even this low (relative to N) O coverage dramatically changes the shape of the TPD peak, shifting the low temperature onset down by about 45 K and high temperature tail down by about 35 K. Further, the well-defined inflection between

states I and II is eliminated, changing the peak shape quite dramatically.

3.5. Modeling: Effect of Oxygen

In order to understand the effect of oxygen in a more quantitative fashion, we modeled the data of Fig. 4 in a manner very similar to that described in Section 3.2. We assume that the effect of oxygen can be accounted for as an oxygen-coverage-dependent modification to the activation energy. Thus, Eq. (1) is modified to

$$-\frac{d\theta}{dt} = \frac{1}{\beta} \Theta_N^n \nu \exp[-(E_a - \alpha_N \Theta_N - \alpha_O \Theta_O)/RT], \quad (2)$$

where α_O is the O coverage dependence of E_a . To fit the data of Fig. 4, we maintained the same parameters that were used for the three N desorption states, adding only the α_O term. Also, we allowed the relative coverages of the three states to vary from that seen for desorption from the pure N surfaces. The fits we achieved for the surfaces with O are of the same quality as those shown in Fig. 2 for N only surfaces. The parameters used for the fitting are listed in Table I.

In Fig. 5 we plot the amount of N in each of the desorption states as a function of N coverage. The filled symbols represent desorption data from surfaces without surface O. The open symbols are for surfaces with a mixture of both N and O. Going from the lowest total coverage to the highest total coverage the individual coverages of O and N for the three oxygen containing surfaces are (1) 0.09 ML N: 0.09 ML O, (2) 0.20 ML N: 0.20 ML O, and (3) 0.47 ML N: 0.10 ML O (estimated—see section 3.2.1). Figure 5 shows that adsorbed oxygen tends to shift desorption out of state I and into states II and III.

4. DISCUSSION

We conducted these experiments with two primary goals in mind. First, we wanted to measure, independent of competing reac-

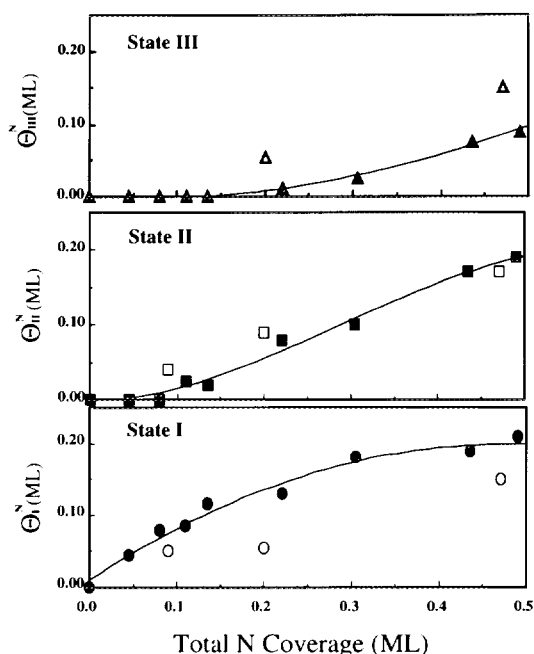


Fig. 5. Amount of N desorbing in a given TPD state vs total N coverage. Closed symbols represent surfaces with nitrogen only. Open symbols are for surfaces with both N and O.

tions, the recombination rate for N atoms at high coverage on Rh(111) to get better rate constants for the $N + N$ reaction. These rate constants are required in order to better understand reactions over Rh surfaces that occur at much higher pressures. Second, we wished to better understand the effect of oxygen on N desorption so that we could rationalize our results with those obtained from NO TPD.

4.1. N_2 Desorption from N Adsorption

4.1.1. Desorption states. Nitrogen atoms recombinatively desorb in multiple desorption states from Rh(111) as is evidenced by the inflections in the desorption data in Figs. 1d–f. Our modeling of those data (see Section 3.2 and Fig. 2) shows that a minimum of three states are present. This conclusion is independent of the specifics of the model used to fit the desorption data (Fig. 1) and is dependent only on the width of and the

inflection points in the desorption spectra at high N coverages. If one fits Fig. 1f ($\Theta_N = 0.49$ ML) using two very broad states, then the parameter set used at $\Theta_N = 0.49$ ML gives very poor fits of the lower coverage ($\Theta_N \leq 0.3$ ML) data. This simple observation is the essence of our conclusion that at least three desorption states are present in our N atom TPD data. It is our viewpoint that three different states result from three distinctly different surface phases and/or ordered structures of N on Rh(111) or from three different N–N near neighbor interactions based on coverage. Unfortunately, the adsorbed N atoms gave no distinctive LEED patterns, nor were we able to detect with HREELS a Rh–N stretch due to N atoms. We feel that it is unlikely that the TPD peaks correspond to different N adsorption sites, since it is generally accepted that N atoms reside in threefold hollow sites (7, 8).

Figure 3 shows how each of the three states fills as the total N coverage is increased. The desorption states fill with a trend that is quite familiar for TPD data exhibiting multiple states. Figure 3 shows that state I is approaching saturation at around 0.2 ML. States II and III, however, show no tendency toward saturation at total surface N coverages of 0.5 ML; therefore, we cannot offer an estimate of the saturation coverages for these two states. To reiterate, although we have obtained the highest atomic N coverages (0.5 ML) ever reported for Rh(111), N uptake in these experiments is most likely limited by our adsorption procedure (Section 2.2) and not by the surface capacity. We speculate that 3/4 ML is more representative of the true saturation coverage for N. In fact, due to the large error in our coverage calibration method, the maximum coverage we obtained could be 0.67 ML. We base our estimate for the “true” saturation N coverage on two previously reported observations. First, Root *et al.* (9) showed that during NO TPD, dissociation of NO led to a surface that contained simultaneously 0.37 ML of N and 0.37 ML of O

for a total surface coverage of 0.74 ML. Second, it is likely that N atom adsorption is similar to O atoms which saturate at 0.83 ML (9).

4.1.2. Rate constants. The primary goal of this paper is to provide rate constants for the N + N reaction that can be used to model reaction kinetics at much higher pressures. In order to extract rate constants from TPD data, modeling is required. In our view, the prudent course is to model the whole desorption spectrum by evaluating the desorption rate equations over the entire temperature and coverage range of the experiment. Using the assumptions set out in Section 3.2.3, we find that a very good fit to our data is achieved when the parameters shown in Table 1 are used. In Fig. 2, the model and data are compared and the quality of fit that we obtain with the model is shown.

The values that we report in Table 1 are consistent with previous papers (9). When comparing to previously reported values, the only meaningful comparison one can make is for desorption in the low coverage limit (state I). For N₂ desorption from low coverages of adsorbed NO, Root *et al.* (9) report $E_a = 31.0$ kcal/mol and $\nu = 3 \times 10^{10}$ s⁻¹, which makes $k^{650\text{ K}} = 1.3$ N₂·s⁻¹. Our state I values in Table 1 give essentially this same value, $k^{650\text{ K}} = 1.28$ N₂·s⁻¹, when evaluated at a low coverage of 0.1 ML. This comparison is good evidence of the validity of our experimental methods and also shows that the N atoms we produce by electron beam dissociation of NO are in fact "the same as" those generated by more traditional methods.

It is important to explicitly spell out the usefulness of the parameters listed in Table 1. Obviously, the values we arrived at are a direct result of our choice to use Eq. (1) as the rate expression and the list of assumptions in Section 3.2.3. Unfortunately, when TPD data of the type we present here are modeled, it is impossible to discriminate our model from several other equally valid formulations. For instance, one might propose

that all of the coverage dependence of the rate constant is in the preexponential. Or one might not restrict all of the reactions to be strictly second order in N coverage. However, regardless of the details of the formulation, all reasonable models must predict the same overall desorption rate at a given temperature and N coverage in order to fit the experimental data. This point is made quite well by the comparison to Root *et al.*'s results given in the preceding paragraph. Further, different models give three states with roughly the same coverages that we present in Fig. 3. Of what use then are the values listed in Table 1? The values provide a good estimate of the desorption rate, from a given state, at a specific N coverage and surface temperature. Strictly speaking, they are only valid over the range of temperatures for which we have desorption data. However, luckily for us this temperature range corresponds quite well to the range of temperatures over which higher pressure kinetic studies for NO reactions have been carried out (4, 5, 17).

4.1.3. Uncertainty in the rate constants. No discussion of the rate constants is complete without some assessment of the uncertainty in those values. In this paper, uncertainty in the rate constants (Table 1) comes primarily from uncertainty in the N coverages. As stated above, we calibrate our coverages relative to the amount of N₂ generated during TPD of saturation NO. Previous papers, combining XPS and TPD measurements, determined that 0.37 ML of N desorbs as N₂ from a surface saturated with NO and then heated to 495 K (9). Since about 40% of the N atoms desorb below 495 K then this result suggests that 0.6 ML of N and 0.6 ML of O are generated during desorption of saturation NO on Rh(111). Total coverages of 1.2 ML during this TPD experiment seem unlikely and we estimate that a more reasonable upper limit is 0.5 ML of N, given that 0.5 ML of O also results from NO dissociation. As a lower limit, we feel that it is unlikely that less than 0.25 ML of N is generated during NO TPD. This

conclusion is based on a comparison of the amount of O that desorbs from an NO-saturated surface with the amount of O that desorbs from an oxygen-saturated surface (9). The error associated with determining the amount of N from NO TPD translates into roughly a factor of 2 error in the coverages in our experiment. Thus, at highest coverage Θ_N is somewhere between 0.34 and 0.67 ML. For our calculations we used 0.49 ML.

The uncertainty in the coverage can be very straightforwardly translated into uncertainty in the rate constant. The following argument applies for all three states listed in Table 1. If in our modeling we have underestimated the N coverage, say that at saturation in Fig. 1 $\Theta_N = 0.67$ ML instead of 0.49 ML, then we must decrease ν and α_N to compensate. All of the preexponentials in Table 1 would be lower by $(0.37/0.67)^2 \approx 0.3$ and the values of α_N would be lower by $(0.37/0.69) \approx 0.5$. Conversely, if we postulate that the maximum coverage in Fig. 1 were 0.34 ML instead of 0.49 ML, then all preexponentials would be increased by $(0.49/0.34)^2 \approx 2$ and the values of α_N would be increased by $(0.49/0.34) \approx 1.4$. Roughly, the maximum uncertainty in the coverage results in about a factor of 7 uncertainty in the rate constant (estimated at 650 K with 0.25 ML N).

4.1.4. Implications for catalysis at higher pressures. Figure 6 compares the N_2 formation rates taken from our TPD experiment (solid lines) to N_2 formation rates measured during reaction of 8 Torr NO with 8 Torr CO (dashed lines) (4). There is excellent agreement between the state II N_2 formation rates and the high pressure reaction data despite the very different environments in which they were measured. In the discussion which follows, we are assuming that the N_2 that is formed during the NO/CO reaction over Rh(111) is generated by an $N + N$ surface reaction. N_2 formation rates for the three TPD states were calculated using the parameters in Table 1, assuming an N coverage of 0.3 ML in each desorption state. The CO/NO reaction rate data was

taken from a previous paper (4). As one can see from Fig. 6, N_2 formation rates from the different desorption states vary by four orders of magnitude. But the important point is that state II desorption parameters best describe the formation rates seen during moderate pressure reactions.

It is clear from Fig. 6 ($\Theta_N = 0.3$ ML) that desorption from state I is 100 times too slow to be an important pathway for N_2 formation under moderate pressure CO/NO reaction conditions (4). Examination of Fig. 3 shows that state I adsorption would in all likelihood be saturated before 0.3 ML; therefore, state I coverages greater than 0.3 ML are not reasonable. Thus, we conclude that reaction of N atoms in the state I surface phase is not responsible for N_2 formation under reaction conditions. The logical extension of the conclusion is that the total surface coverage must be high enough to give significant coverages in at least state II. This sets a lower limit of $\Theta_N = 0.25$ ML under reaction conditions.

Looking now at state III desorption we can say that if the coverage of this state were 0.3 ML, then N_2 would be formed about $50 \times$ faster than the N_2 formation rate under reaction conditions. State III desorption rates are comparable to the measured N_2 formation rates under reaction conditions when $\theta_{III} \approx 0.04$ ML. The data in Fig. 3 suggest that this would occur when the $\theta_{total} \approx 0.40$ ML, $\theta_I \approx 0.20$ ML, and $\theta_{II} \approx 0.15$ ML. Under these conditions N_2 formation due to states II and III would be comparable. Thus, we can *not* completely eliminate state III as a pathway for N_2 formation under reaction conditions; however, the coverage in state III would be quite small and the surface N atoms would have to be simultaneously desorbing from both states II and III. Although concurrent desorption from multiple states is well known for TPD measurements where both surface temperature and nitrogen coverage are changing simultaneously, we feel that under steady-state reaction conditions at high pressures all of the surface N atoms are equivalent

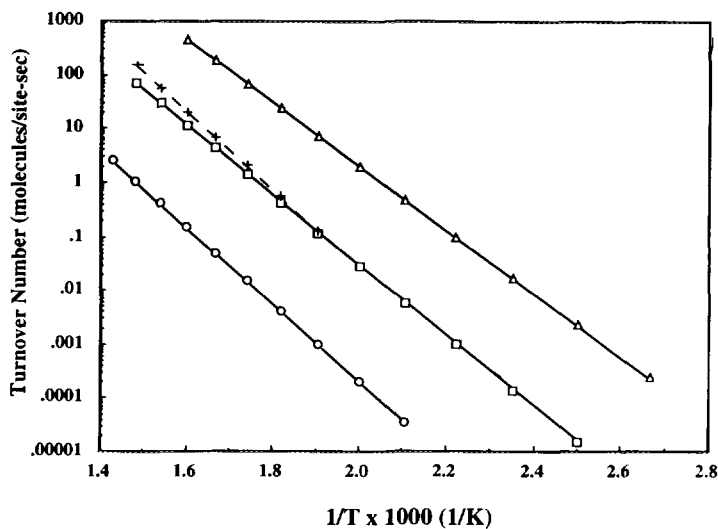


FIG. 6. Calculated desorption rate from each TPD state vs $1/T$ at a fixed N coverage of 0.3 ML in each state. Circles represent the state I desorption rate, squares are for state II, and triangles are for state III. Included for comparison are the + symbols and dashed lines which are the measured N₂ formation rates over Rh(111) using 8 Torr of Co and 8 Torr of NO.

and therefore desorb at the same rate. Provided all surface N are equivalent, only state II N desorption can explain the high pressure data. Thus, our results suggest that under the reaction conditions to which we are making a comparison, the N coverage is not saturated but instead is somewhere between 0.25 and 0.6 ML. These speculations must be checked by detailed modeling. We present them here primarily to show how the data we are reporting fit in with previously measured moderate pressure reaction data. However, two conclusions can be put forth. First, N atom recombination most likely occurs via the state II desorption pathway. Second, N atom recombination is not inherently rate-limiting under reaction conditions. At high N coverage the N + N reaction is $50\times$ faster than the observed N₂ production rate. Therefore, N₂ production must be limited by N atom coverage as a result of either limited NO dissociation and/or NO adsorption.

4.2. Effects of O

We examined the effect of oxygen in order to get a more quantitative estimate of how

adsorbed oxygen alters the N + N reaction rate. These data also help rationalize our N atom TPD data with N₂ desorption from NO adsorption where both N and O are present (9). The data in Figs. 4 and 5 show two ways that oxygen affects N₂ desorption. First, it increases the desorption rate out of state I quite significantly. In our model, 0.2 ML of adsorbed O lowers the state I desorption barrier by 3 kcal/mol; this increases the state I desorption rate by roughly a factor of 10 at 650 K. As a result of this increased state I desorption rate the high temperature N₂ desorption edge shifts to lower temperature and decreases the separation of states I and II. State II and III rate constants are not strongly altered by O within the coverage range we examined. The effect of oxygen may be to force nitrogen atoms into high coverage islands of atomic N at lower coverages than on the nitrogen only surfaces.

The second effect of oxygen is to increase the population of the lower temperature states in comparison to similar N coverages without oxygen. This is best illustrated by Fig. 5, where the open symbols represent

the data taken on surfaces with coadsorbed N and O. As is evident from the figure, adding oxygen to surface pushes N out of state I and into state III. State II populations are only mildly affected. This effect explains why our low coverage activation energy is somewhat higher than that previously determined based on NO TPD measurements (9).

4.3. Comparison with NO TPD

It is important that we relate our finding to previously reported N₂ desorption data (9). The most significant comparison that can be made is to N₂ desorption from NO adsorption (9). Our results are very consistent with these previous findings. When NO is adsorbed on Rh(111), N₂ from the N + N reaction is reported to desorb in a single broad desorption peak (9), as opposed to the three peaks we report here. The important difference between our data and those NO TPD data is that equal amount of N and O are present on the surface when the N desorbs as N₂ from adsorbed NO. In that paper (9) and this one, it is shown that oxygen strongly affects the N₂ desorption spectrum, primarily by shifting state I desorption to lower temperature. As a result of this shift states I and II overlap much more strongly and are no longer visually distinguishable.

5. SUMMARY

We have studied the N atom recombination reaction over Rh(111) using TPD and kinetic modeling. By using *e*⁻ beam dissociation of adsorbed NO, we obtained the highest N atom coverages on Rh(111) yet obtained. Our TPD data show that N atoms recombinatively desorb in at least three distinct desorption states. Comparison our results with previous measurements of the CO/NO reaction at 16 Torr total pressure shows that under reaction conditions N atom recombination most likely occurs via the state II desorption pathway from a surface that is *not* saturated with N atoms. We

estimate that N atom coverages are between 0.25 and 0.6 ML. Also, N atom recombination is not inherently rate-limiting under reaction conditions. At high N coverage the N + N reaction is 50× faster than that observed under reaction conditions. Some other process, either NO dissociation and/or NO adsorption, must limit the N coverage, which in turn limits the N₂ production rate.

ACKNOWLEDGMENTS

The authors gratefully thank Galen Fisher of GM Research for the use of the chamber and for his encouragement and helpful discussions. We also thank Se Oh for his many useful comments. In addition, we thank Dusan Velic of Wayne State University for his assistance in the early set-up of this experiment. K.Y.S. Ng acknowledges partial financial support from General Motors Research during his sabbatical leave to perform this research.

REFERENCES

1. Taylor, K. C., *Chemtech* **20**, 551 (1990).
2. Taylor, K. C., "Automobile Catalytic Converters." Springer-Verlag, Berlin, 1984.
3. Taylor, K. C., *Catal. Rev.*, in press.
4. Belton, D. N., and Schmieg, S. J., *J. Catal.* **144**, 9 (1993).
5. Oh, S. H., Fisher, G. B., Carpenter, J. E., and Goodman, D. W., *J. Catal.* **100**, 360 (1986).
6. Fisher, G. B., Oh, S. H., DiMaggio, C. L., Schmieg, S. J., Goodman, D. W., and Peden, C. H. F., Chem. Inst. of Canada, Ottawa, 1988.
7. Root, T. W., Fisher, G. B., and Schmidt, L. D., *J. Chem. Phys.* **85**, 4679 (1986).
8. Root, T. W., Fisher, G. F., and Schmidt, L. D., *J. Chem. Phys.* **85**, 4687 (1986).
9. Root, T. W., Schmidt, L. D., and Fisher, G. B., *Surf. Sci.* **134**, 30 (1983).
10. Daniel, W. M., Kim, Y., Peebles, H. C., and White, J. M., *Surf. Sci.* **111**, 349 (1982).
11. Zafiris, G. S., and Gorte, R. J., *J. Catal.* **132**, 275 (1991).
12. Altman, E. I., and Gorte, R. J., *J. Catal.* **113**, 185 (1988).
13. Sexton, B. A., *J. Vac. Sci. Technol. A* **16**, 1033 (1979).
14. Fisher, G. B., and Schmieg, S. J., *J. Vac. Sci. Technol. A* **1**, 1064 (1983).
15. King, D. S., *Surf. Sci.* **47**, 384 (1975).
16. Boudart, M., "Kinetics of Chemical Processes." Prentice-Hall, Englewood Cliffs, NJ, 1968.
17. Peden, C. H. F., Goodman, D. W., Blair, D. S., Fisher, G. B., Berlowitz, P. J., and Oh, S. J., *J. Phys. Chem.* **92**, 1563 (1988).